

1 **Novel Sustainable Carbon Dot as Dual Replacements for**
2 **Emulsion Stabilizers and Photoinitiators in Macroporous**
3 **Polymerized High Internal Phase Emulsion Fabrication**

4 **Woming Gao^{1*}, Zeming Cheng^{1,2}, Nicholas T.H. Farr^{1,2}, Cornelia Rodenburg^{1,2*}, Frederik Claeysens^{1,2*}**

5 * Corresponding authors

6
7 ¹School of Chemical, Materials and Biological Engineering, Sir Robert Hadfield Building, University
8 of Sheffield, Sheffield, S1 3JD, UK

9 ²Insigneo Institute for in Silico Medicine, Pam Liversidge Building, University of Sheffield, S1 3JD,
10 UK

11
12 **Keywords:** carbon dots; emulsion stabilizer; photoinitiator; macroporous PolyHIPEs; enlarged
13 pore throats; fluid permeability; cell permeability

14
15
16
17
18
19
20
21
22
23
24
25
26
27
28
29
30
31
32
33
34
35
36
37
38
39

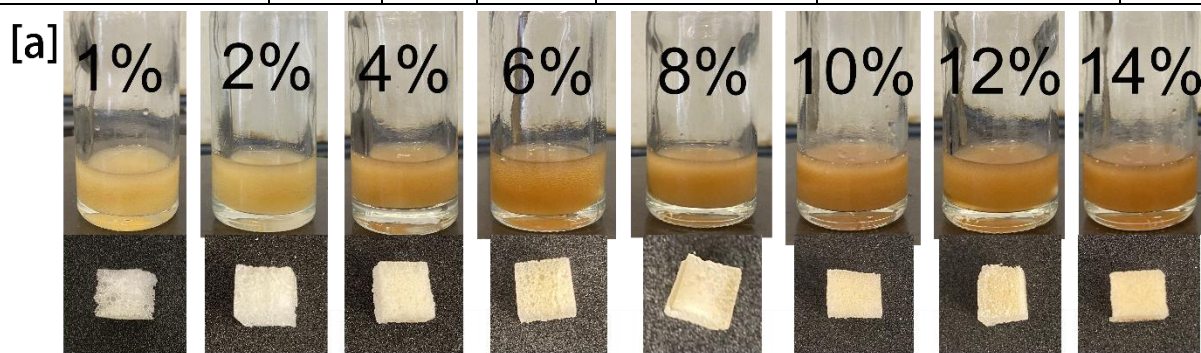
40 **Complementary Results**

41 **PolyHIPEs emulsion stability time and polymerization rate**

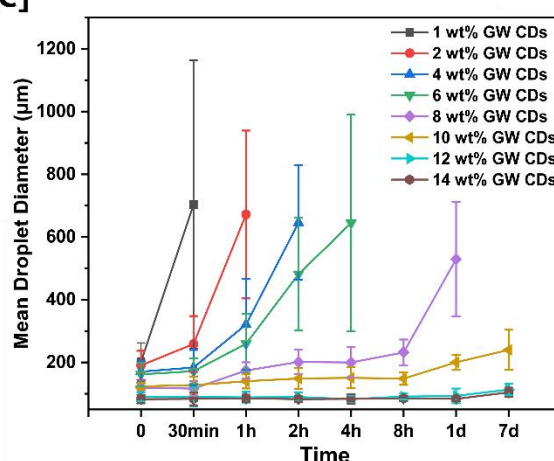
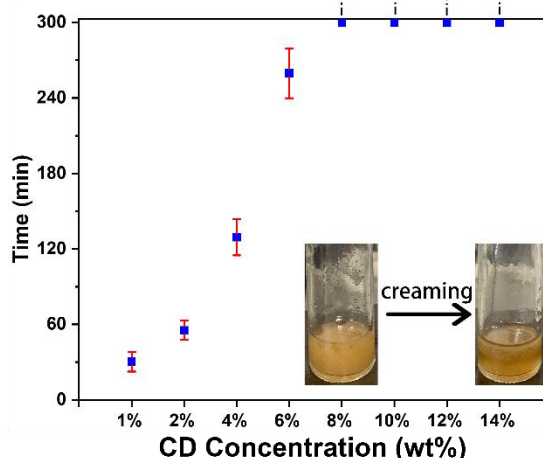
42

43 **Table S1. Material composition of various PolyHIPEs (20 vol% organic phase, 80 vol% water phase)**

	Orangic phase			Carbon dots	Conventional emulsion stabilizer/photoinitiator	
	EHA (wt%)	IBOA (wt%)	TMPTA (wt%)	GW CDs (wt% ratio in Organic phase)	Hypermer B246 (wt% ratio in Organic phase)	TPO (wt% ratio in Organic phase)
1% GW CDs-PolyHIPE	42	42	16	1	-	-
2% GW CDs-PolyHIPE	42	42	16	2	-	-
4% GW CDs-PolyHIPE	42	42	16	4	-	-
6% GW CDs-PolyHIPE	42	42	16	6	-	-
8% GW CDs-PolyHIPE	42	42	16	8	-	-
10% GW CDs-PolyHIPE	42	42	16	10	-	-
12% GW CDs-PolyHIPE	42	42	16	12	-	-
14% GW CDs-PolyHIPE	42	42	16	14	-	-
4% Hypermer/TPO-PolyHIPE	42	42	16	-	4	4



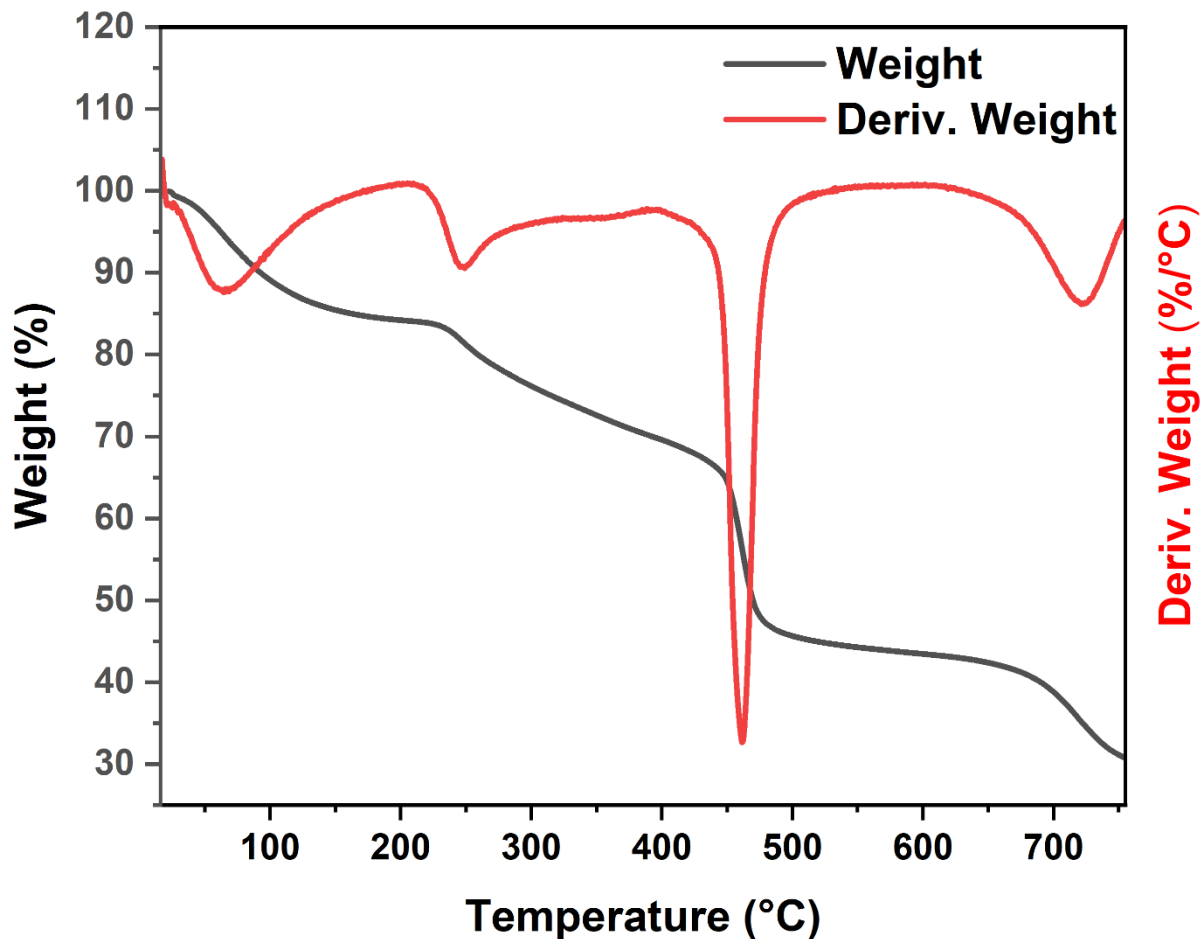
[b]



44

45 **Figure S1. (a) Stable emulsions containing different GW CDs mass ratios and their cured PolyHIPEs. (b)**
46 **The stability time of each emulsion. (c) Long-term emulsion stability of emulsions stabilized with varying**
47 **concentrations of GW CDs.**

48 Thermogravimetric Analysis (TGA) of GW CDs



49
50 Figure S2.TGA spectrum of GW CDs.

51 **O1s XPS spectrum and detailed XPS spectra of GW CDs**

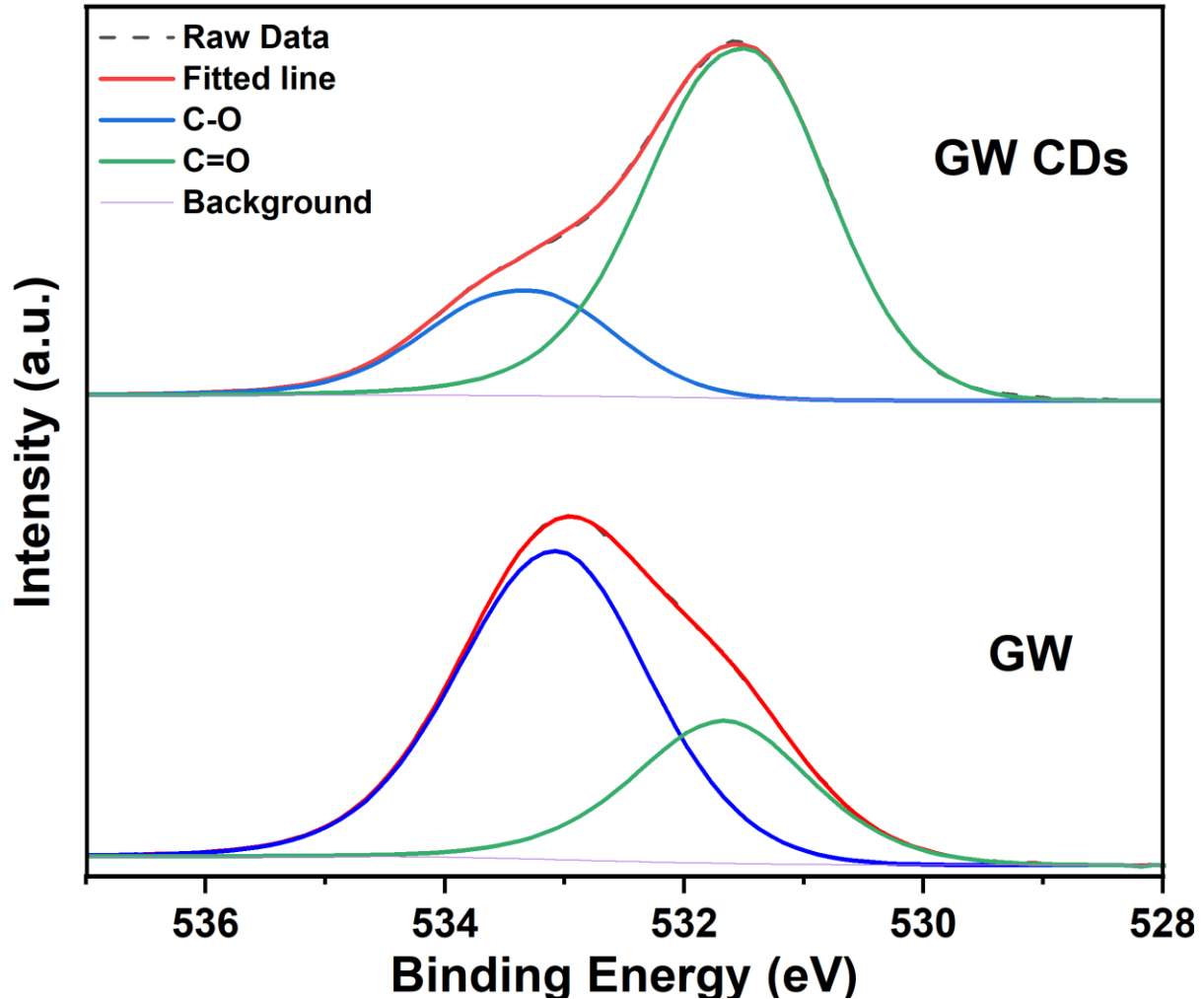


Figure S3. O1s XPS spectra of GW and GW CDs.

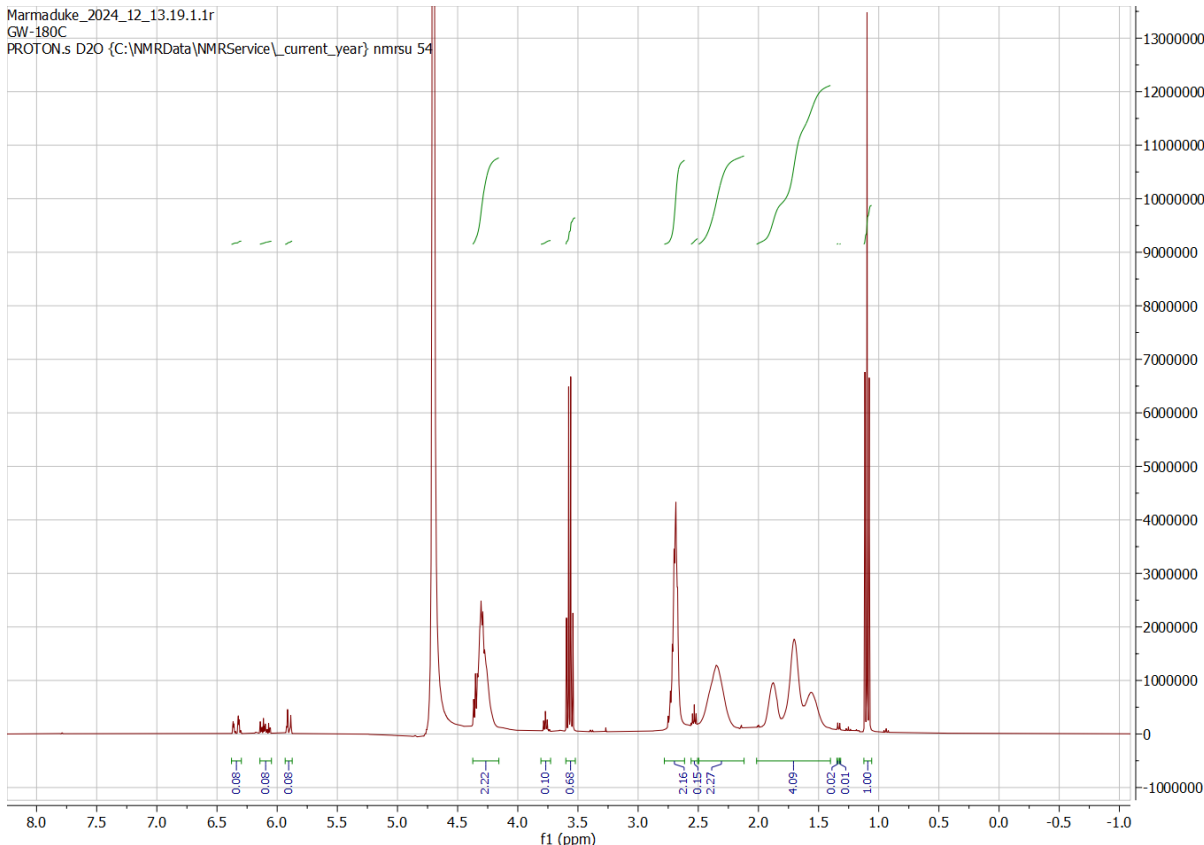
55 **Table S2. The contents of each element and group in GW CDs obtained by full XPS spectrum and high-
56 resolution C1s and O1s XPS spectra.**

		GW CDs (%)	Gromwell root waste (%)
Full Spectrum	O	29.13	27.45
	N	1.18	1.98
	Ca	3.73	3.73
	K	0.85	0.19
	C	63.58	66.99
	Si	-	1.47
	Al	-	0.68
C1s	sp^3 C/ sp^2 C	38.49	48.06
	C-O	29.92	18.87
	C-N	6.42	20.01
	C=O/O-C=O	22.64	12.55
	π - π^* satellite	2.53	0.5

O1s	C-O	38.22	69.71
	C=O	61.78	30.29

57

58 HLB test of GW CDs



59

60 **Figure S4.** ^1H NMR spectrum of GW CDs and the integration of each peak, with the peak at 1.15 ppm as
61 the reference peak (area = 1)

62

63

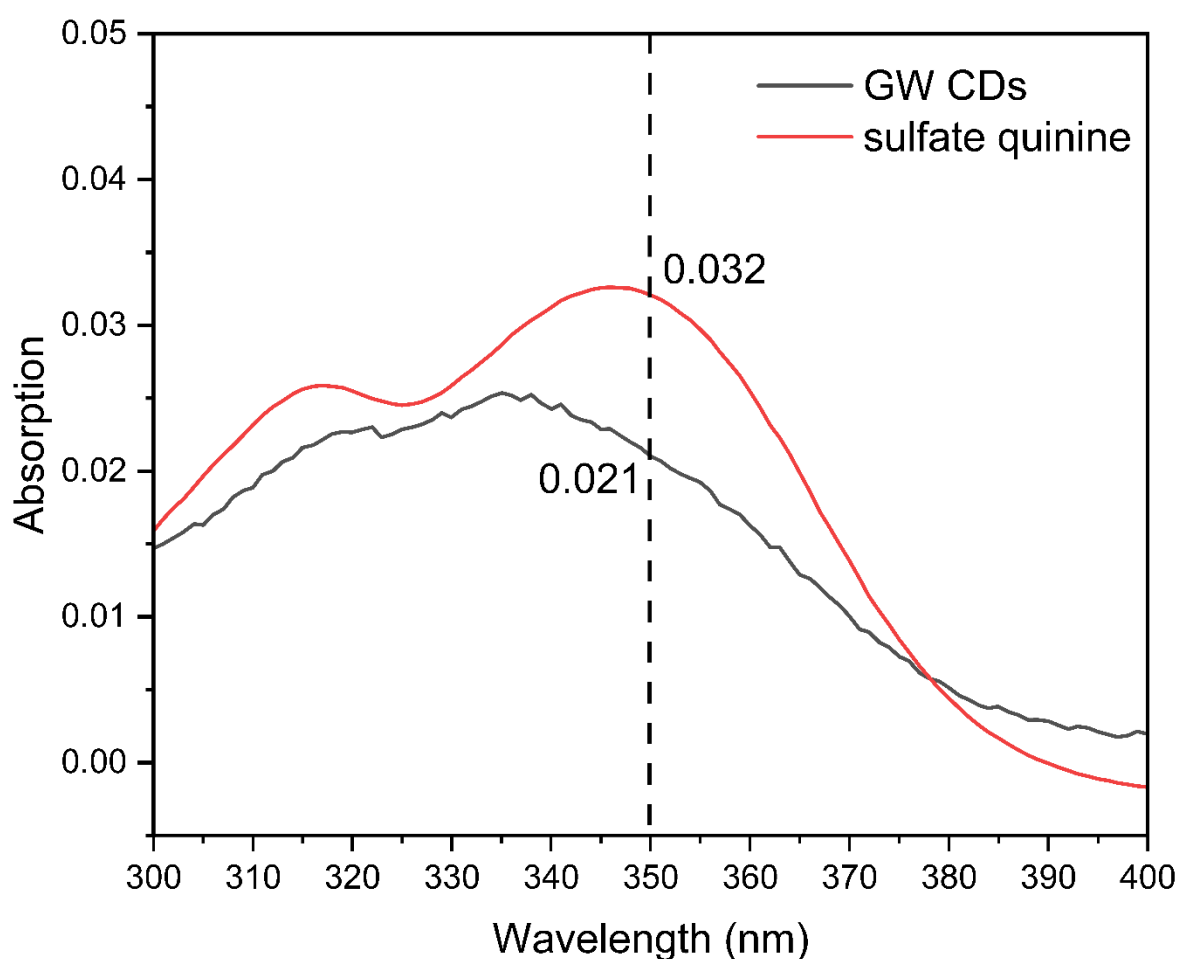
Table S3. Integration of hydrophilic and hydrophobic peaks in ^1H NMR and calculated HLB of GW CDs

Hydrophobic groups		Hydrophilic groups	
Signal (ppm)	Integration	Signal (ppm)	Integration
<1	0.03	3.2-3.3	0.01
1-1.15	1	2.6-2.8	2.22
1.15-1.3	0.11	3.5-3.6	0.65
1.3-1.4	0.06	3.72-3.8	0.1
1.4-2.1	4.12	4.15-4.4	2.31
2.1-2.5	2.28		
2.5-2.56	0.19		
5.87-6.38	0.26		
Total	8.05	Total	5.29

According to the formula 2, HLB= 7.39

64

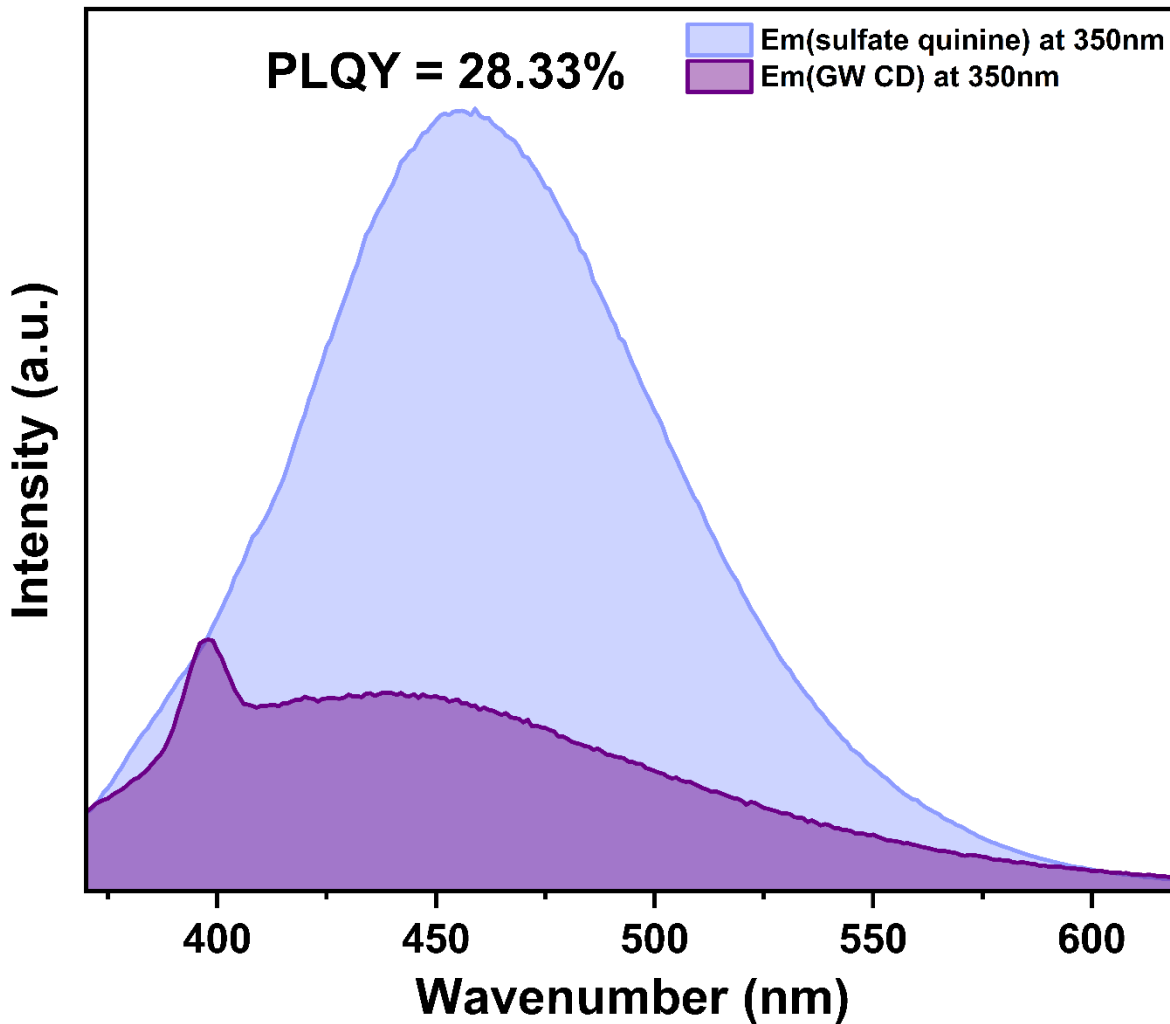
65 **PLQY test of GW CDs**



66

67 **Figure S5. Comparison of the absorbance of quinine sulfate solution and GW CDs solution under 350nm**
68 **UV light. The absorbance less than 0.1 can be regarded as the same refractive index.**

69



70

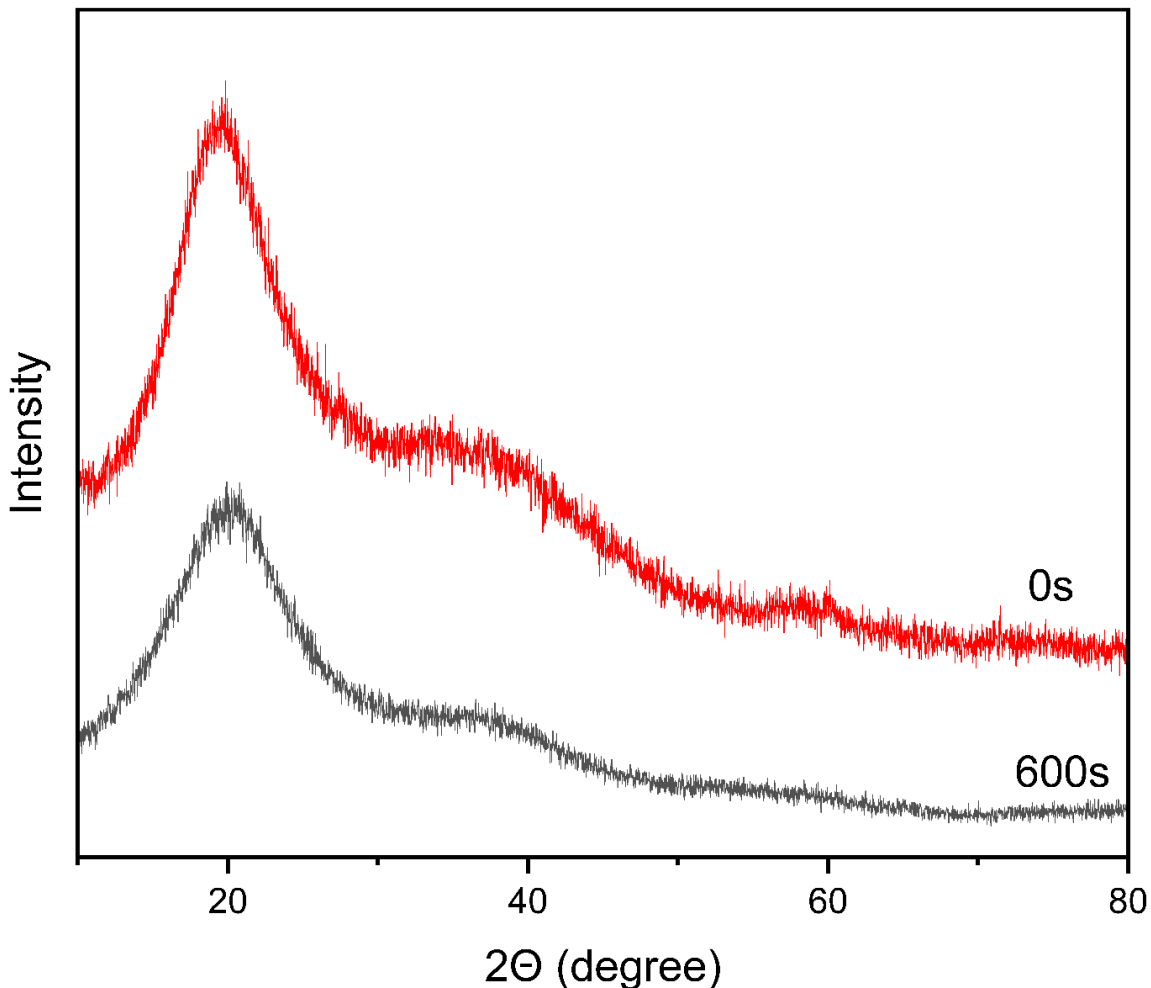
71 Figure S6. Comparison of the fluorescence emission intensities of quinine sulfate solution and GW CDs
 72 solution under 350nm UV light. The absorbance less than 0.1 can be regarded as the same refractive index.

73 According to the formula 3 and figure S5, $\frac{A_{QS}}{A_{GW\,CDs}} = 1.524$, $\frac{S_{GW\,CDs}}{S_{QS}} = 0.344$, $PLQY_{GW\,CDs} = 28.33\%$

74

75

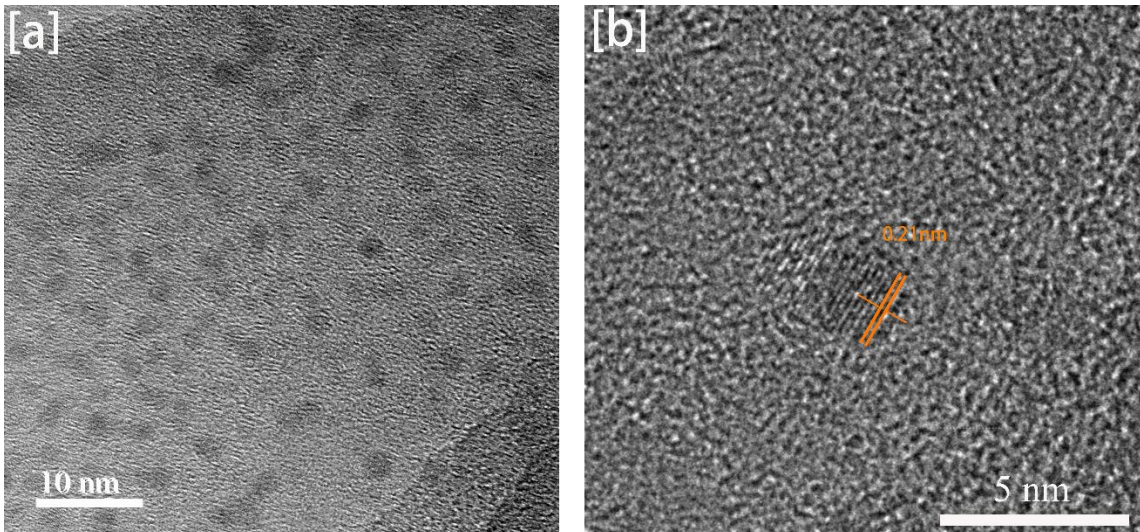
76 **XRD of GW CDs before and after UV Exposure**



77 **Figure S7. XRD of GW CDs before and after UV irradiation.**

78

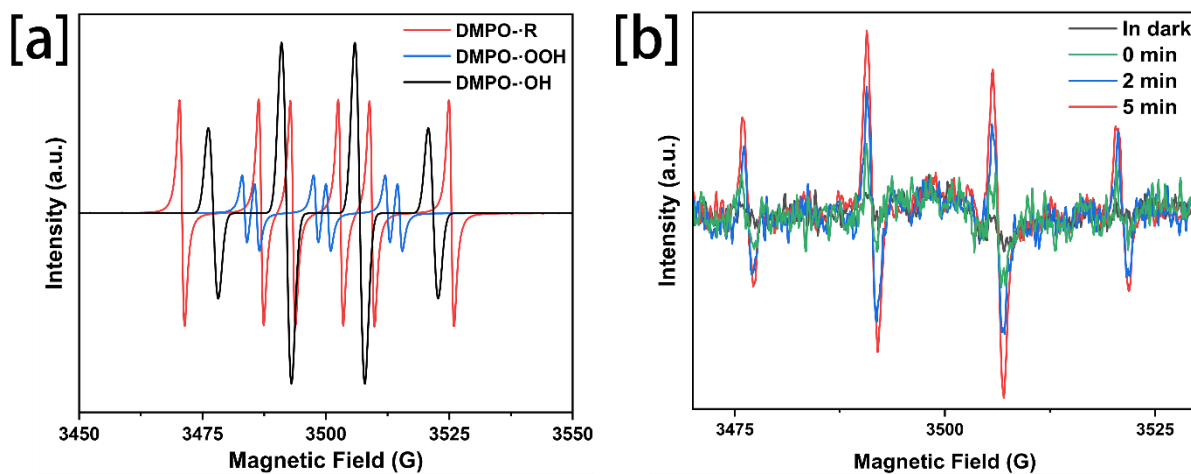
79 **TEM Pictures of GW CDs after UV Exposure**



80 **Figure S8. TEM image (a) of GW CDs after UV irradiation for 600s and high-resolution TEM image (b) of**
81 **GW CDs.**

82

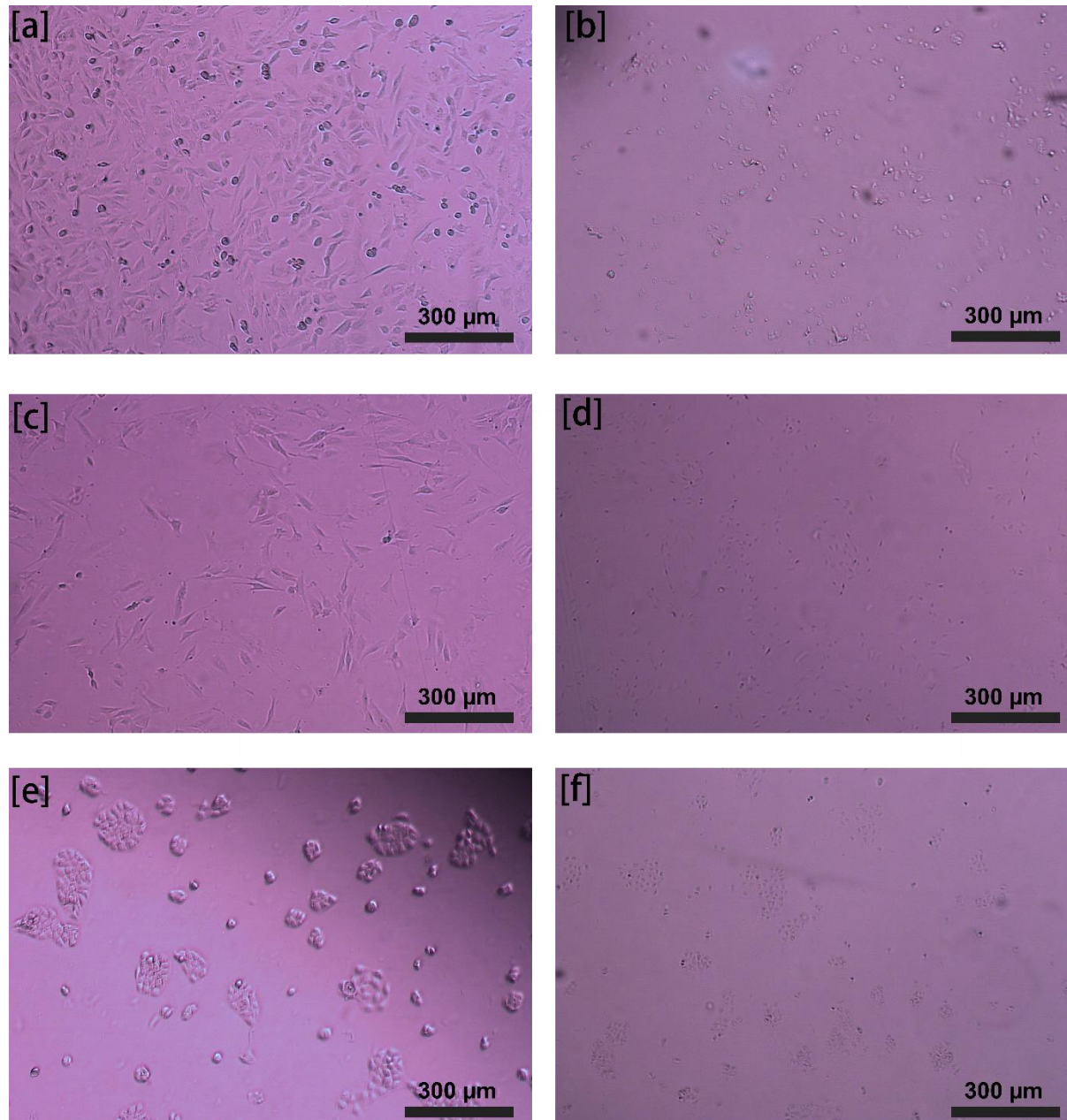
83 **Simulated EPR spectra, EPR spectrum of GW CDs aqueous solution**
84 **after oxygen removal and EPR spectra of prepolymer/GW CDs**
85 **ethanol solution**



86 **Figure S9. (a): Simulated EPR spectra trapped by the DMPO provided by the program Easyspin.**
87 **Simulations resulted in DMPO-OH: $g = 2.00592$, $A_N = 14.9$ G, and $A_H = 14.9$ G. DMPO-R: $g = 2.00592$, $A_N =$**
88 **16.0 G, and $A_H = 23.3$ G. DMPO-OOH: $g = 2.00592$, $A_N = 12.0$ G, and $A_H = 2.5$ G. (b): EPR spectra of**
89 **radicals trapped by DMPO in deoxygenated water under 365 nm UV irradiation for varying durations,**
90 **cGW CDs=10 mg/mL, cDMPO = 4 mg/mL.**

91
92

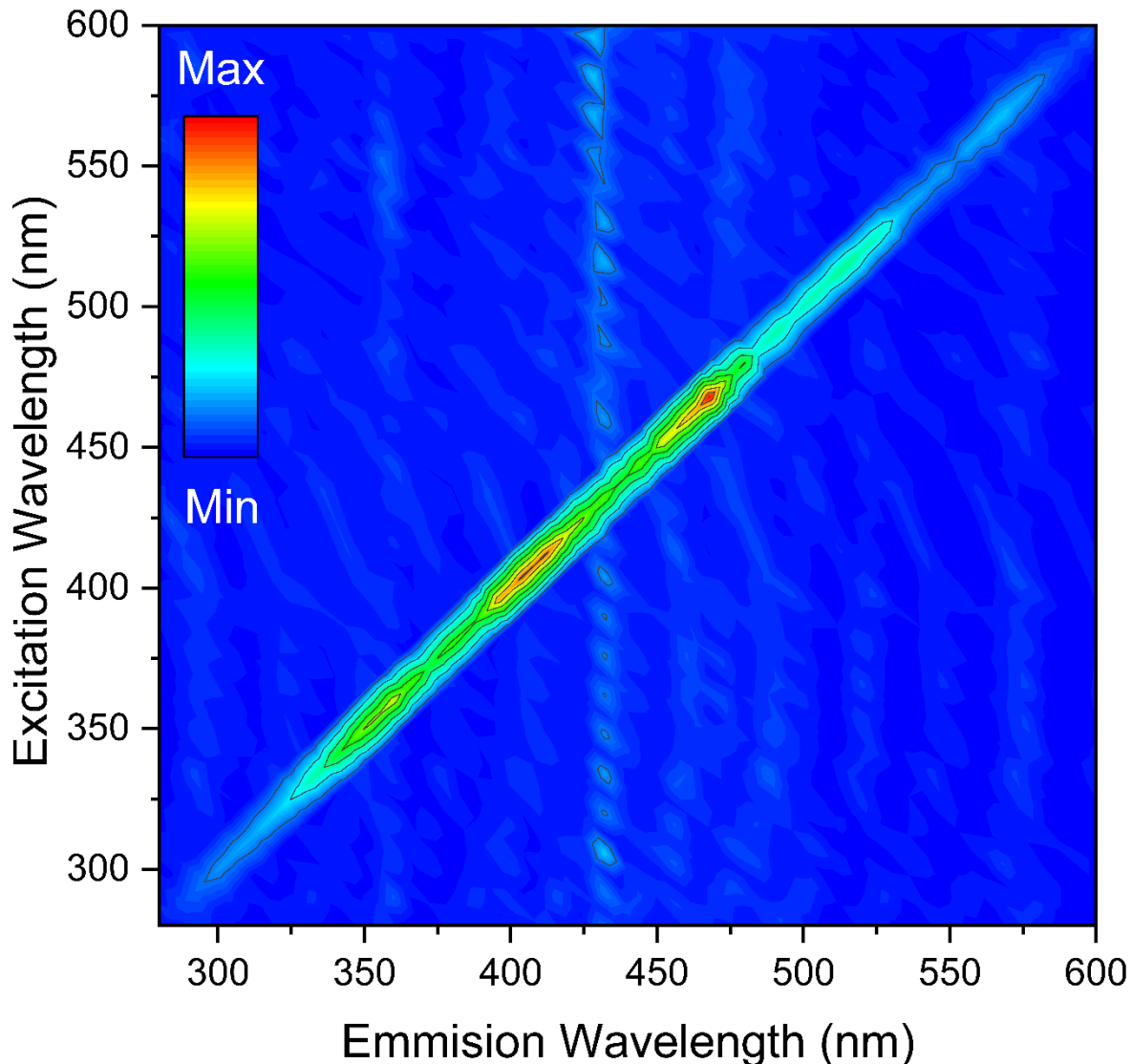
93 The morphology comparation of cells in media containing GW CDs
94 and Hypermer B246/TPO



95
96 **Figure S10.** The morphology of BJ5TA cells in media containing GW CDs (a) and Hypermer B246/TPO (b)
97 with 10 \times magnification. The morphology of MLO-A5 cells in media containing GW CDs (c) and Hypermer
98 B246/TPO (d) with 10 \times magnification. The morphology of HaCaT cells in media containing GW CDs (e)
99 and Hypermer B246/TPO (f) with 10 \times magnification. All the scale bar is 300 μ m.

100
101
102
103
104

105 The EEM of GW CDs without Rayleigh and Raman scattering
106 removed



107
108 Figure S11. EEM of GW CDs without Rayleigh and Raman scattering removed

109 The average pore size, the average number of pore throats per pore,
110 and the average pore throat diameter for each PolyHIPE sample.

111
112 Table S4. The average pore diameter, the average number of pore throats per pore, and the average pore
113 throat diameter of each PolyHIPE sample.

	The average pore size (μm)	The average number of pore throats per pore	The average pore throat diameter (μm)
1% GW CDs-PolyHIPE	834±498	4.3±1.7	121±62

2% GW CDs-PolyHIPE	588±363	2.8±1.5	105±73
4% GW CDs-PolyHIPE	363±161	4.7±1.7	89±52
6% GW CDs-PolyHIPE	310±111	2.6±1.5	64±33
8% GW CDs-PolyHIPE	231±86	2.8±1.3	62±42
10% GW CDs-PolyHIPE	186±63	1.5±1.3	56±25
12% GW CDs-PolyHIPE	167±40	1±0.7	31±10
14% GW CDs-PolyHIPE	144±24	0.1±0.0	35±19
4% Hypermer/TPO-PolyHIPE	51±8	16.1±8.0	3±2

114

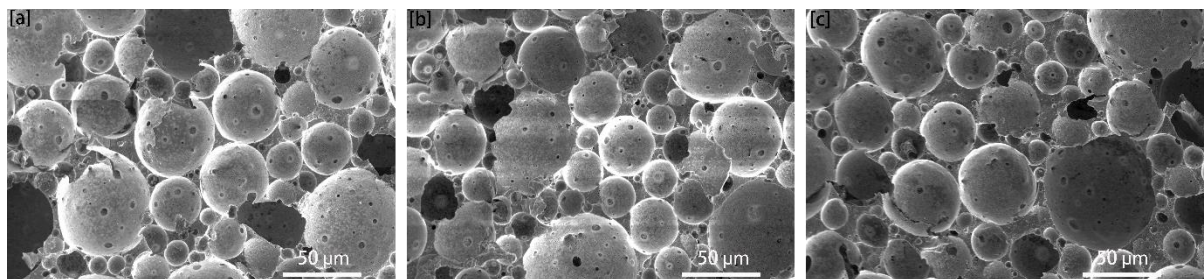
115 **The average droplets diameter of each GW CDs-stabilized emulsion
116 at different temperatures.**

117

118 **Table S5. The average droplets diameter of each GW CDs-stabilized emulsion at 20, 45 and 70 °C.**

	The average droplets size (μm) at 20 °C	The average droplets size (μm) at 45 °C	The average droplets size (μm) at 70 °C
1% GW CDs-PolyHIPE	258±63	537±117	901±189
2% GW CDs-PolyHIPE	218±45	428±88	633±122
4% GW CDs-PolyHIPE	174±23	258±44	383±53
6% GW CDs-PolyHIPE	129±20	211±29	322±37
8% GW CDs-PolyHIPE	103±12	160±22	245±29
10% GW CDs-PolyHIPE	93±15	137±14	203±21
12% GW CDs-PolyHIPE	89±7	120±9	171±13
14% GW CDs-PolyHIPE	86±5	104±6	121±11

119

120 **The SEM image of 2%, 6%, 8% Hypermer/TPO-PolyHIPE**

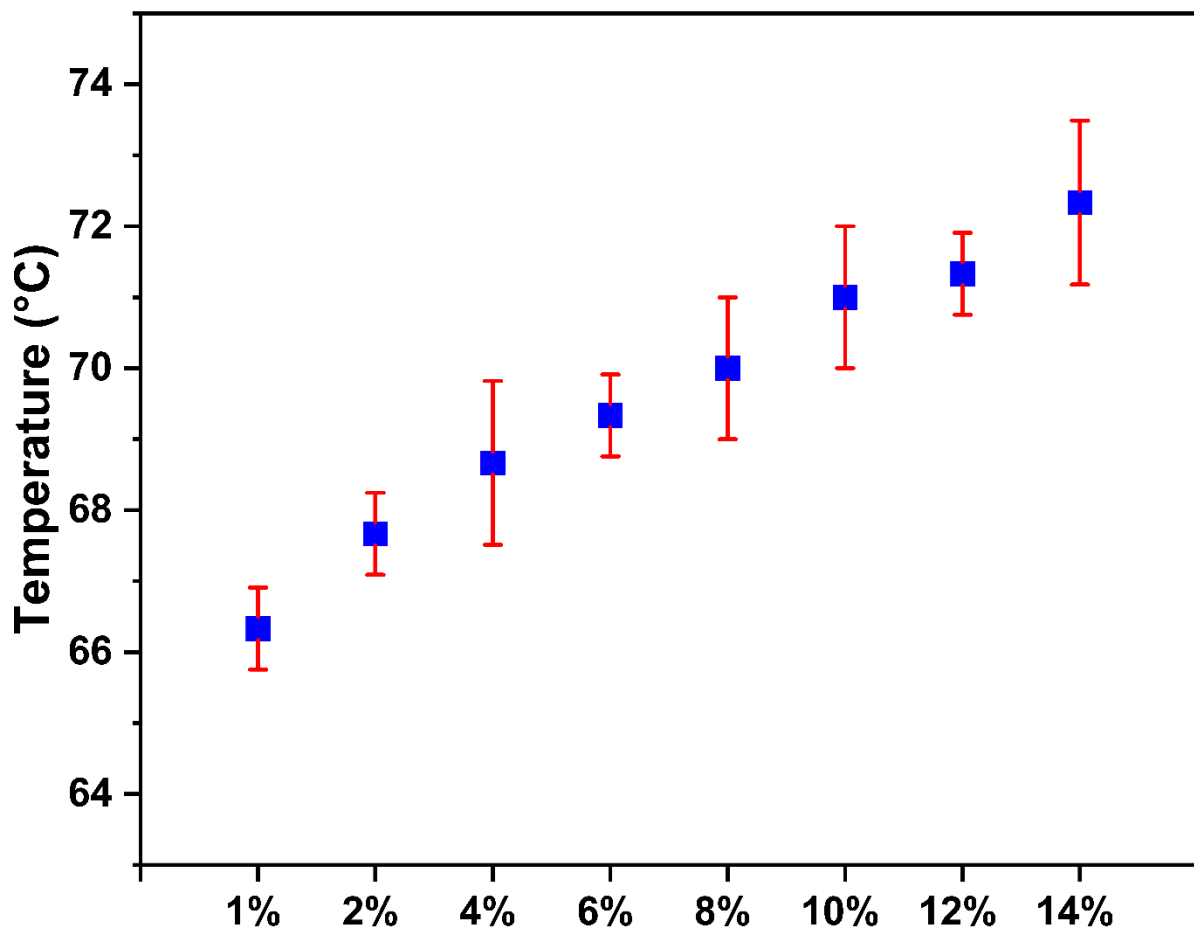
121

122 **Figure S12. SEM images of PolyHIPE samples containing 2 wt% (a), 6 wt% (b), 8 wt% (c) Hypermer B246
123 and TPO. All the scale bar is 50 μm.**

124

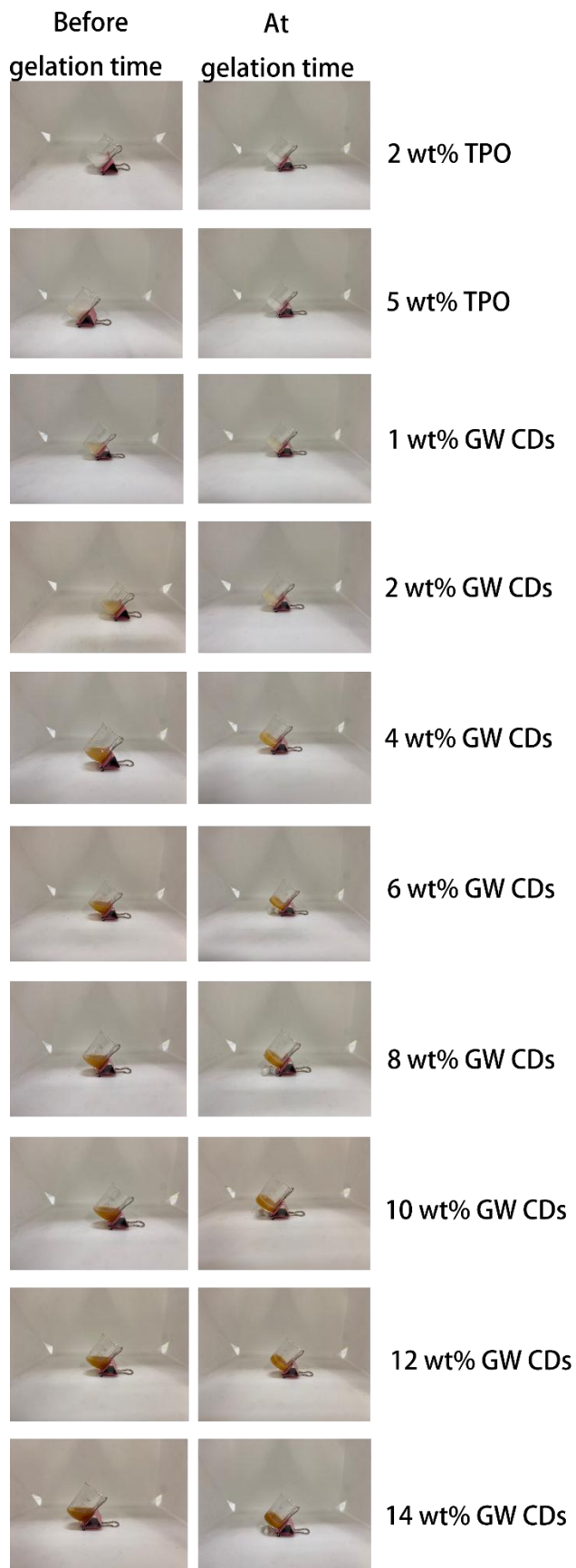
125

The surface temperature of the PolyHIPEs after curing



126

127 **Figure S13.** The surface temperature of each GW CDs-stabilized PolyHIPEs after 180 seconds of curing
128 under 365 nm UV light at an intensity of 1700 mW/cm². PolyHIPE samples containing 1 wt%, 2 wt%, 4
129 wt%, 6 wt%, 8 wt%, 10 wt%, 12% wt% and 14 wt% GW CD were abbreviated into 1%, 2%, 4%, 6%, 8%, 10%,
130 12%, 14% in figures.



131

132

133

Figure S14. Images of emulsions containing various GW CDs and TPO concentrations, captured both before and at the gelation point.

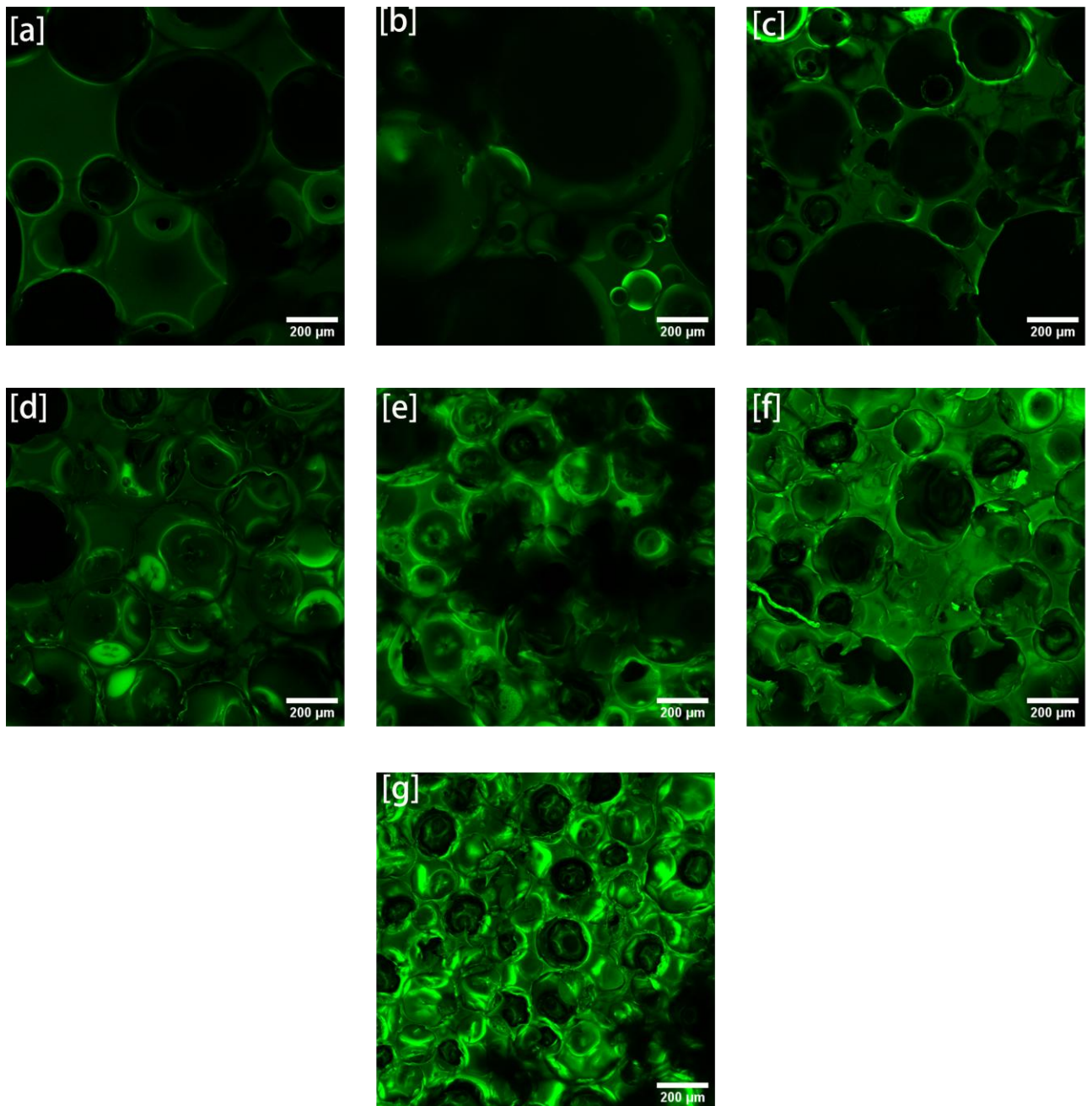
134

135

Table S6. Total curing enthalpy (ΔH) measured by photo-DSC tests during PolyHIPE photocuring.

	The total curing enthalpy (ΔH) (J/g)
1% GW CDs-PolyHIPE	4.02
2% GW CDs-PolyHIPE	4.06
4% GW CDs-PolyHIPE	4.08
6% GW CDs-PolyHIPE	4.32
8% GW CDs-PolyHIPE	4.33
10% GW CDs-PolyHIPE	4.61
12% GW CDs-PolyHIPE	4.67
14% GW CDs-PolyHIPE	5.16
2% TPO-PolyHIPE	5.44
5% TPO-PolyHIPE	4.38

136



137

138

Figure S15. The confocal images of 1, 2, 4, 6, 8, 10, 12 wt% GW CDs-PolyHIPE under 488 nm excitation wavelength.

139

140

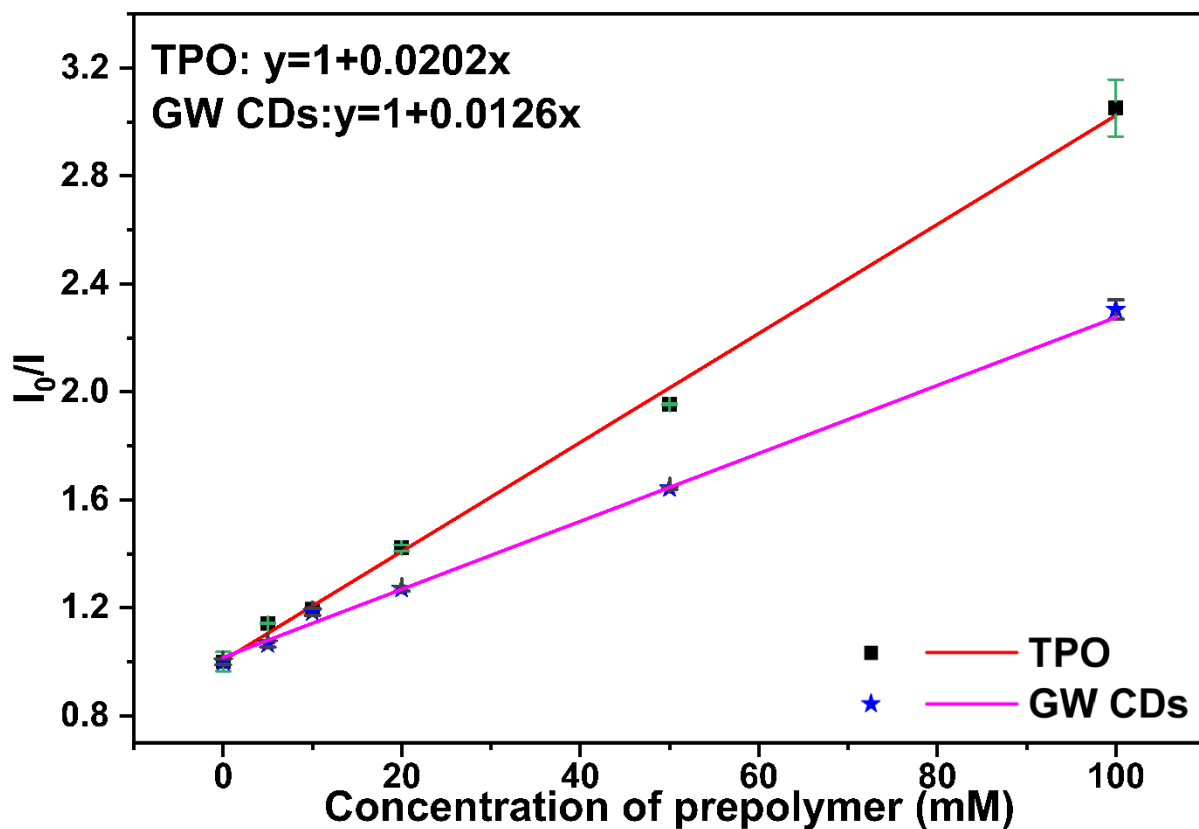
141

Table S7. The average droplets diameter of each GW CDs-stabilized emulsion in long-term stability test.

	The average droplets size (μm) at							
	0 min	30 min	1 h	2 h	4 h	8 h	1 day	7 days
1% GW CDs-PolyHIPE	202 ± 60	704 ± 460	creamed	-	-	-	-	-
2% GW CDs-PolyHIPE	190 ± 46	259 ± 89	672 ± 268	creamed	-	-	--	--
4% GW CDs-	171 ± 34	184 ± 56	321 ±	646 ±	creamed	-	-	-

PolyHIPE			145	183				
6% GW CDs-PolyHIPE	162 ± 37	172 ± 41	259 ± 95	481 ± 180	644 ± 346	creamed	-	--
8% GW CDs-PolyHIPE	119 ± 14	117 ± 24	174 ± 26	201 ± 39	200 ± 49	232 ± 41	529 ± 183	creamed
10% GW CDs-PolyHIPE	123 ± 11	128 ± 27	140 ± 23	149 ± 33	151 ± 33	148 ± 20	200 ± 24	240 ± 64
12% GW CDs-PolyHIPE	91 ± 14	91 ± 30	88 ± 18	90 ± 15	83 ± 12	91 ± 9	93 ± 23	113 ± 18
14% GW CDs-PolyHIPE	83 ± 13	84 ± 20	85 ± 12	83 ± 10	85 ± 8	84 ± 8	84 ± 8	105 ± 15

142



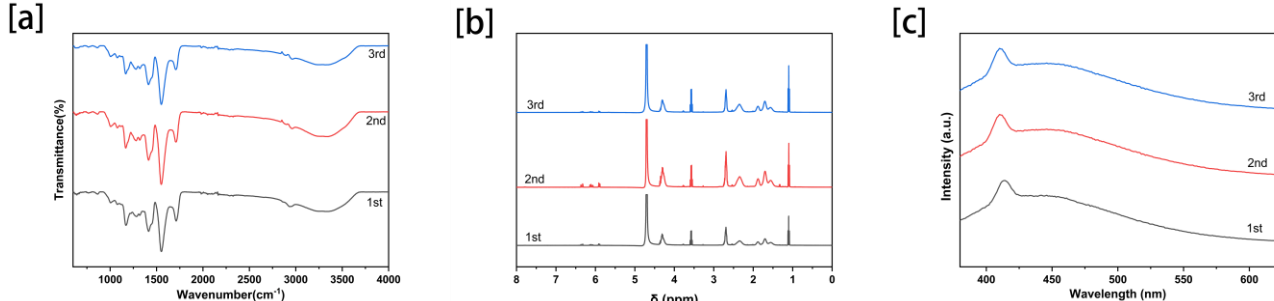
143

144

Figure S16. Stern-Volmer plots of fluorescence quenching of TPO (black squares) and GW CDs (blue stars) by the EHA/IBOA/TMPTA prepolymer mixture in ethanol.

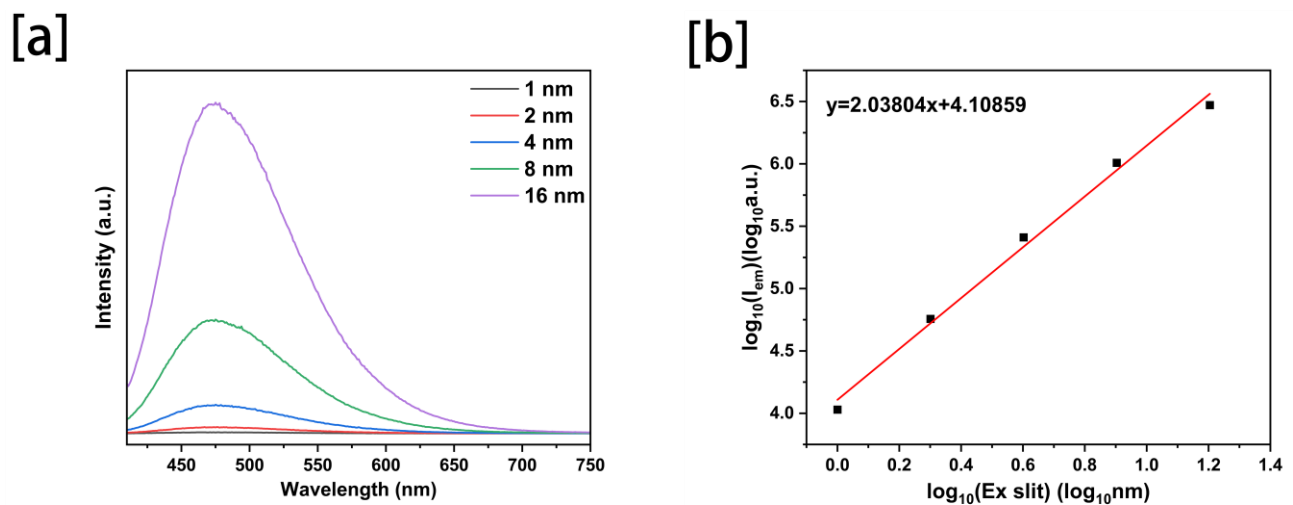
145

146



147

148 **Figure S17. FTIR (a), NMR (b) and PL emission spectra (c) to test the batch-to-batch reproducibility of GW**
149 **CDs prepared in three independent syntheses (1st-3rd).**



150

151 **Figure S18. Influence of excitation slit width on the PL intensity of GW CDs (a) and corresponding up-**
152 **conversion analysis (b).**

153

154